Continuum functional methods to study strong-QCD in new generation facilities

Jorge Segovia

INP at Nanjing University, and
Pablo de Olavide University, Seville

Perceiving the Emergence of Hadron Mass through AMBER@CERN

CERN, Switzerland, 30 March - 2 April, 2020

Quantum Chromodynamics in its non-perturbative regime

Emergence

Low-level rules producing high-level phenomena with enormous apparent complexity

Start from the QCD Lagrangian:

$$\mathcal{L}_{\text{QCD}} = -\frac{1}{4} G_a^{\mu\nu} G^a_{\mu\nu} + \frac{1}{2\xi}(\partial^\mu A^a_\mu)^2 + \partial^\mu \bar{c}^a \partial_\mu c^a + g\, f^{abc}(\partial^\mu \bar{c}^a) A^b_\mu c^c + \text{quarks}$$

Lattice-regularized QCD, Continuum Schwinger-function methods, ...

And obtain:

- Dynamical generation of fundamental mass scale in pure Yang-Mills (gluon mass).
- Quark constituent masses and spontaneous chiral symmetry breaking.
- Bound state formation: mesons, baryons, glueballs, hybrids, multiquark systems...
- Signals of confinement.

Non-perturbative QCD (strong-QCD) is a multifaceted problem whose solution demands multipronged analysis from many different directions

Non-perturbative QCD: Dynamical generation of gluon mass

☞ Dressed-gluon propagator in Landau gauge:

$$i\Delta_{\mu\nu} = -iP_{\mu\nu}\mathbf{\Delta(q^2)}, \quad P_{\mu\nu} = g_{\mu\nu} - q_\mu q_\nu / q^2$$

- An inflexion point at $q^2 > 0$.
- Breaks the axiom of reflexion positivity.
- Gluon mass generation $\leftrightarrow$ Schwinger mechanism.

A.C. Aguilar *et al.*, Phys. Rev. D78 (2008) 025010;
I.L. Bogolubsky *et al.*, Phys. Lett. B676 (2009) 69.

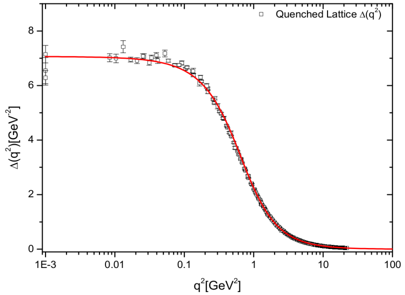

☞ Dressed-ghost propagator in Landau gauge:

$$G^{ab}(q^2) = \delta^{ab}\,\frac{\mathbf{J(q^2)}}{q^2}$$

- No power-like singular behavior at $q^2 \to 0$.
- Good indication that $J(q^2)$ reaches a plateau.
- Saturation of ghost's dressing function.

Ph. Boucaud *et al.*, JHEP 0806 (2008) 099;
C. Fischer *et al.*, Annals Phys. 324 (2009) 2408.

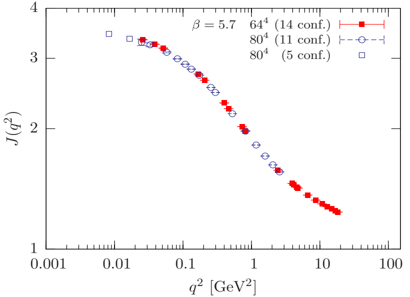

Non-perturbative QCD: Saturation at IR of process-independent effective-charge

D. Binosi *et al.*, Phys. Rev. D96 (2017) 054026;
A. Deur *et al.*, Prog. Part. Nucl. Phys. 90 (2016) 1-74.

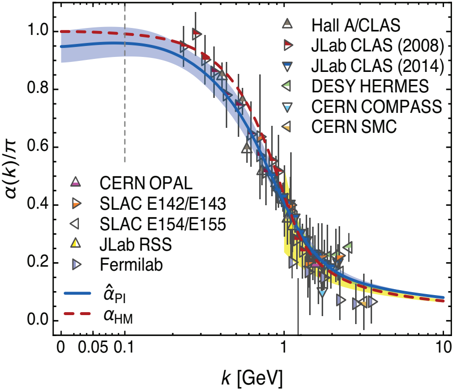

- Data = running coupling defined from the Bjorken sum-rule.

$$\int_0^1 dx \left[g_1^p(x,k^2) - g_1^n(x,k^2)\right] = \frac{g_A}{6}\left[1 - \frac{1}{\pi}\alpha_{g_1}(k^2)\right]$$

- Curve determined from combined continuum and lattice analysis of QCD's gauge sector (massless ghost and massive gluon).
- The curve is a running coupling that does NOT depend on the choice of observable.
  - No parameters.
  - No matching condition.
  - No extrapolation.
- It predicts and unifies an enormous body of empirical data via the matter-sector bound-state equations.

- Perturbative regime:

$$\alpha_{g_1}(k^2) = \alpha_{\overline{MS}}(k^2)\left[1 + 1.14\alpha_{\overline{MS}}(k^2) + \dots\right]$$

$$\hat{\alpha}_{PI}(k^2) = \alpha_{\overline{MS}}(k^2)\left[1 + 1.09\alpha_{\overline{MS}}(k^2) + \dots\right]$$

☞ Dressed-quark propagator in Landau gauge:

$$S^{-1}(p) = Z_2(i\gamma\cdot p + m) + \Sigma(p) = \left(\frac{Z(p^2)}{i\gamma\cdot p + \mathbf{M(p^2)}}\right)^{-1}$$

- Mass generated from the interaction of quarks with the gluon-medium.
- Light quarks acquire a HUGE constituent mass.
- Responsible of the 98% of proton's mass, the large splitting between parity partners, ...

M.S. Bhagwat *et al.*, Phys.Rev. C68 (2003) 015203.

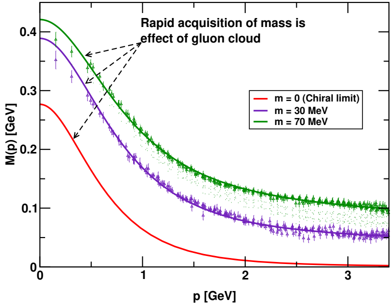

☞ Goldberger-Treiman relation at the quark level:

Quark propagator: $S^{-1}(p) = i\gamma\cdot p\,A(p^2) + B(p^2)\,,$

Pion's BS-amplitude: $\Gamma_\pi(p,P) \propto \gamma^5 E_\pi(p;P)\,.$

$$\mathbf{f_\pi E_\pi(p;0) = B(p^2)}$$

Properties of the massless pion are a direct measure of the dressed-quark mass function

Cleanest expression of the mechanism that is responsible for almost all the visible mass in the universe

Diquark correlations

Any interaction capable of creating Goldstone modes as bound-states of light dressed $q\bar{q}$ will necessarily generate strong $\bar{3}_c$ correlations between any two dressed quarks.

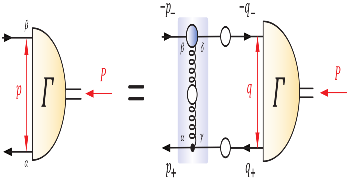

Meson BSE

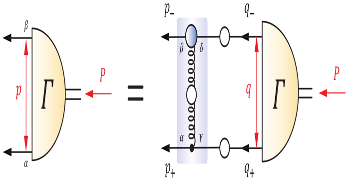

Diquark BSE

☞ Owing to properties of charge-conjugation, a diquark with spin-parity J^P may be viewed as a partner to the analogous J^{-P} meson:

$$\Gamma_{q\bar{q}}(p;P) = - \int \frac{d^4q}{(2\pi)^4}\, g^2 D_{\mu\nu}(p-q)\frac{\lambda^a}{2}\gamma_\mu\, S(q+P)\Gamma_{q\bar{q}}(q;P)S(q)\,\frac{\lambda^a}{2}\,\gamma_\nu$$

$$\Gamma_{qq}(p;P)C^\dagger = -\frac{1}{2}\int \frac{d^4q}{(2\pi)^4}\, g^2 D_{\mu\nu}(p-q)\frac{\lambda^a}{2}\gamma_\mu\, S(q+P)\Gamma_{qq}(q;P)C^\dagger S(q)\,\frac{\lambda^a}{2}\,\gamma_\nu$$

☞ Whilst no pole-mass exists, the following mass-scales express the strength and range of the correlation:

$$m_{[ud]_{0^+}} = 0.7-0.8\,\text{GeV}, \quad m_{\{uu\}_{1^+}} = 0.9-1.1\,\text{GeV}, \quad m_{\{dd\}_{1^+}} = m_{\{ud\}_{1^+}} = m_{\{uu\}_{1^+}}$$

☞ Diquark correlations are soft, they possess an electromagnetic size:

$$r_{[ud]_{0^+}} \gtrsim r_\pi, \qquad r_{\{uu\}_{1^+}} \gtrsim r_\rho, \qquad r_{\{uu\}_{1^+}} > r_{[ud]_{0^+}}$$

Octet and decuplet baryons

	[nn]	{nn}	[ns]	{ns}	{ss}
N	●	●			
Δ		●			
Λ	●		●	●	
Σ		●	●	●	
Ξ			●	●	●
Ω					●

Other baryons as parity partners

- $[I = 0, J^P = 0^+]$: Isoscalar-scalar.
- $[I = 1, J^P = 1^+]$: Isovector-pseudovector.
- $[I = 0, J^P = 0^-]$: Isoscalar-pseudoscalar.
- $[I = 0, J^P = 1^-]$: Isoscalar-vector.
- $[I = 1, J^P = 1^-]$: Isovector-vector.

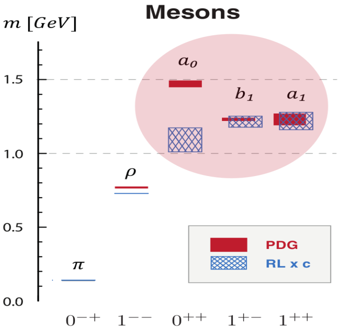

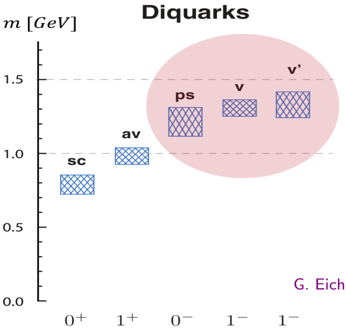

G. Eichmann *et al.*

The quark+diquark structure of a baryon

☞ A baryon can be viewed as a **Borromean bound-state**, the binding within which has two contributions:

- Formation of tight diquark correlations.
- Quark exchange depicted in the shaded area.

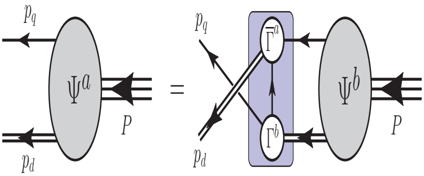

☞ The exchange ensures that diquark correlations within the baryon are fully dynamical: no quark holds a special place.

☞ The rearrangement of the quarks guarantees that the baryon's wave function complies with Pauli statistics.

☞ The number of states in the spectrum of baryons obtained is similar to that found in the three-constituent quark model, just as it is in today's LQCD calculations.

☞ Modern diquarks are different from the old static, point-like diquarks which featured in early attempts to explain the so-called missing resonance problem.

☞ Modern diquarks enforce certain distinct interaction patterns for the singly- and doubly-represented valence-quarks within the baryon.

S.-S. Xu *et al.*, Phys. Rev. D92 (2015) 114034; Y. Lu *et al.*, Phys. Rev. C96 (2017) 015208;
C. Chen *et al.*, Phys. Rev. D100 (2019) 054009; P.-L. Yin *et al.*, Phys. Rev. D100 (2019) 034008.

Three-quark cf. quark-diquark

G. Eichmann *et al.*, Phys. Rev. D94 (2016) 094033;
Few-Body Syst. 58 (2017) 81;
Prog. Part. Nucl.Phys. 91 (2016) 1-100.

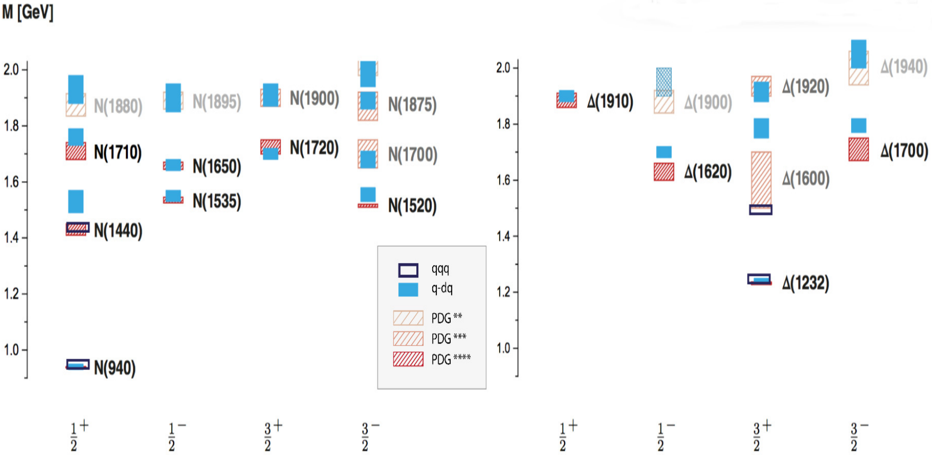

- Spectrum in one to one agreement with experiment.
- Correct level ordering (without coupled-channels effects).
- Three-body agrees with quark-diquark where applicable.

Other kind of two-body correlations?

☞ Hybrid mesons: Existence of strong two-body correlations in the gluon-quark, $q_g = [gq]$, and gluon-antiquark, $\bar{q}_g = [g\bar{q}]$ channels.

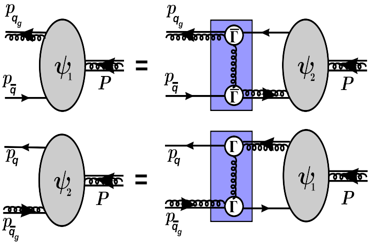

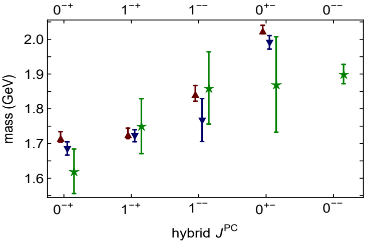

S.S.- Xu *et al.*, Eur. Phys. J. A Lett. 55 (2019) 113.

☞ Glueballs: The infrared suppression of the three-gluon bertex is essential to achieve agreement with lattice-QCD predictions for the 0^{-+} glueball mass.

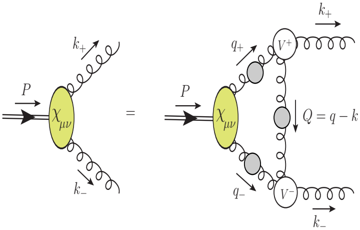

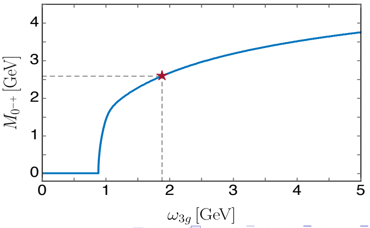

E.V. Souza *et al.*, Eur. Phys. J. A56 (2020) 25.

- Black solid curves are the Pion and Kaon elastic form factors computed at leading order in the symmetry-preserving scheme for bound-state equations.

- Red-dotted curves are the leading-order, leading-twist hard scattering formula

$$Q^2 F_M(Q^2) \overset{Q^2 > Q_0^2}{\approx} 16\pi\alpha_s(Q^2) f_M^2 w_M^2(Q^2)\,,$$

  where $w_M^2(Q^2)$ is related with the meson's PDA and we are using its conformal limit $\varphi^{\rm cl}(x) = 6x(1-x)$.

- Dashed curves are the same formulae but using continuum approach to the kaon and pion PDAs, appropriate to the scale of the experiment.

- Acc. to 25% on $Q^2 \approx 8\,\text{GeV}^2$, becoming more reliable as $\ln Q^2$ is increased.

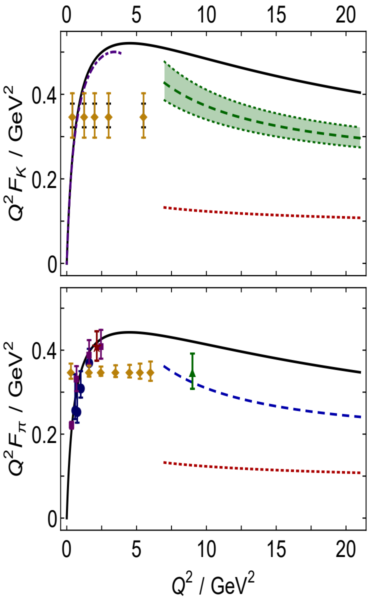

A.C. Aguilar *et al.*, Eur. Phys. J. A55 (2019) 190;
F. Gao *et al.*, Phys. Rev. D96 (2017) 034024.

- A QCD process-independent effective charge, which saturates at IR momenta:
  - Introduce an unambiguous definition of an hadronic scale, $\xi_H \sim 0.3 - 0.5\,\text{GeV}$.
  - Compute *e.g.* the pion's parton distribution functions at such scale.
  - Evolve them to the region of interest.
- Evolved to $\xi_5 = 5.2\,\text{GeV}$, the calculated distribution agrees with that obtained in a recent lQCD computation (grey).
- It also agrees with π-nucleon Drell-Yan data (purple), rescaled by the complete next-to-leading-order (NLO) reanalysis.
- Importantly, via evolution, we also deliver realistic predictions for the pion's glue (green) and sea (red) content.
- Ratio of valence u-quark PDFs in the pion and the kaon at ξ_5. Dashed, solid, and dot-dashed curves represents, respectively, 0, 5%, 10% of the kaon's light-front momentum carried by glue at ξ_H.

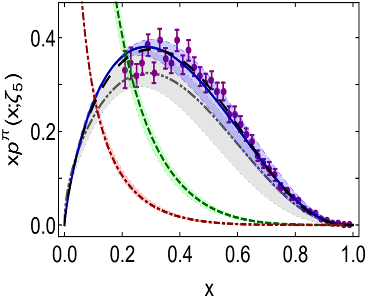

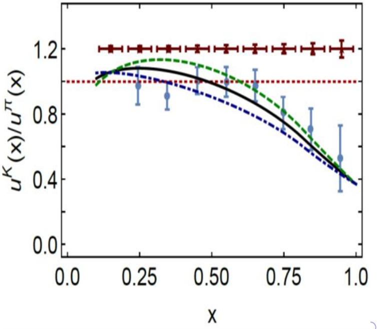

A.C. Aguilar *et al.*, Eur. Phys. J. A55 (2019) 190;
M. Ding *et al.*, Chin. Phys. 44 (2020) 031002.

Barycentric plots: *left panel* – conformal limit PDA, $\varphi_N^{\rm cl}([x]) = 120 x_1 x_2 x_3$; *middle panel* – computed proton PDA evolved to $\zeta = 2\,$GeV, which peaks at $([x]) = (0.55, 0.23, 0.22)$; and *right panel* – Roper resonance PDA at $\zeta = 2\,$GeV. The white circle in each panel serves only to mark the centre of mass for the conformal PDA, whose peak lies at $([x]) = (1/3, 1/3, 1/3)$.

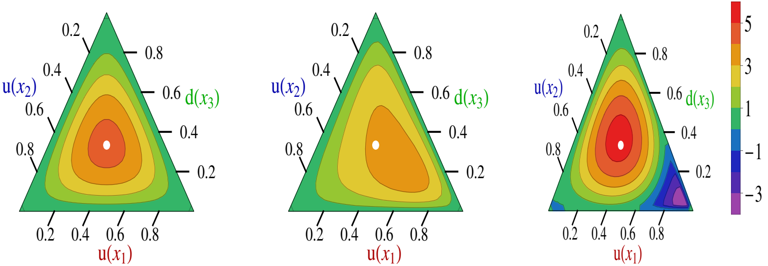

☞ Observations:

- Proton: The leading-twist PDA of the ground-state nucleon is both broader than $\varphi_N^{\rm cl}([x])$ and decreases monotonically away from its maximum in all directions.
- Proton: The peak of the φ-distribution is shifted toward the region where the single quark carries most of the nucleon light-cone momentum fraction.
- Roper: The excitation's PDA is not positive definite which echos features of the wave function for the first radial excitation of a quantum mechanical system.

C. Mezrag *et al.*, Phys. Lett. B783 (2018) 263.

Structure functions: Nucleon and Roper PDAs (II)

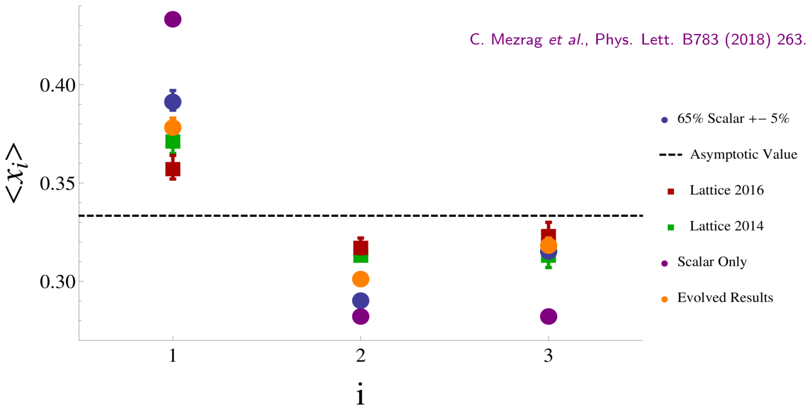

	Scalar	S+AV	Evolved	Braun:2014wpa	Bali:2015ykx
$\langle x_1 \rangle_\varphi$	0.434	0.392(5)	0.379(4)	0.372(7)	0.358(6)
$\langle x_2 \rangle_\varphi$	0.283	0.291(2)	0.302(1)	0.314(3)	0.319(4)
$\langle x_3 \rangle_\varphi$	0.283	0.316(4)	0.319(3)	0.314(7)	0.323(6)
$10^3\, f_N$ (GeV^2)	2.97	4.05	3.78(14)	2.84(33)	3.60(6)

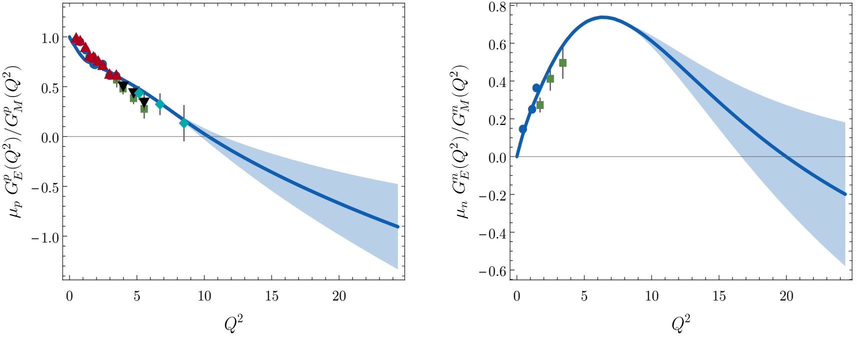

☞ Observations:

- There is no evidence for scaling in Dirac and Pauli form factors, and thus in the electromagnetic Sach form factors.
- Our analysis predicts a zero for the proton's electromagnetic ratio at $Q^2 = 10.3^{+1.1}_{-0.7}$ GeV^2.
- The neutron's electromagnetic ratio has a peak at $Q^2 \approx 6\,\text{GeV}^2$ and then crossed zero for $Q^2 = 20.1^{+10.6}_{-3.5}$ GeV^2.
- All these features can be related with both quark-quark and angular momentum correlations within the nucleon.

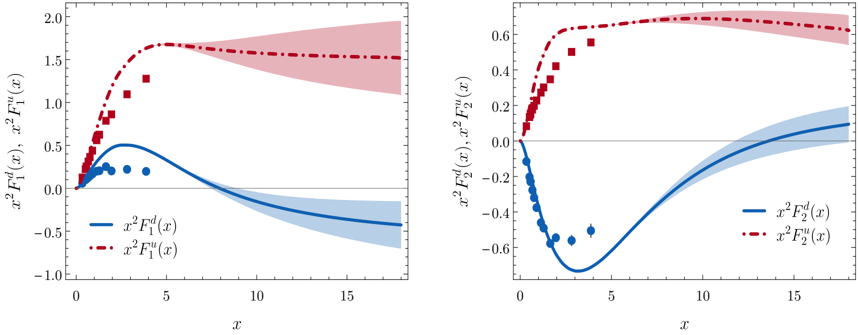

☞ Observations:

- F_1^d is smaller than F_1^u, even allowing for the difference in normalisation, and decreases more quickly as x increases.
- The location of the zero in F_1^d is a measure of the relative probability of finding pseudovector and scalar diquarks in the proton.
- The u- and d-quark Pauli form factors are roughly equal in magnitude on $x \lesssim 5$; *i.e.* F_2^d is suppressed with respect F_2^u but only at large momentum transfer.
- There are contributions playing an important role in F_2, like the anomalous magnetic moment of dressed-quarks or meson-baryon final-state interactions.

Transition Dirac form factor of $\gamma^* N \to N(1440)\frac{1}{2}^+$

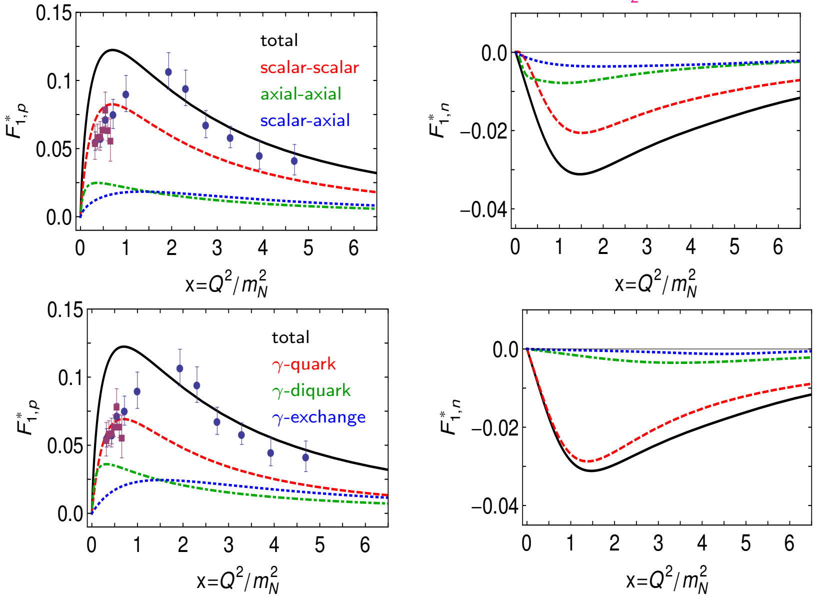

C. Chen *et al.*, Phys. Rev. D99 (2019) 034013.

Structure functions: electro-production of nucleon resonances (II)

Transition Pauli form factor of $\gamma^* N \to N(1440)\frac{1}{2}^+$

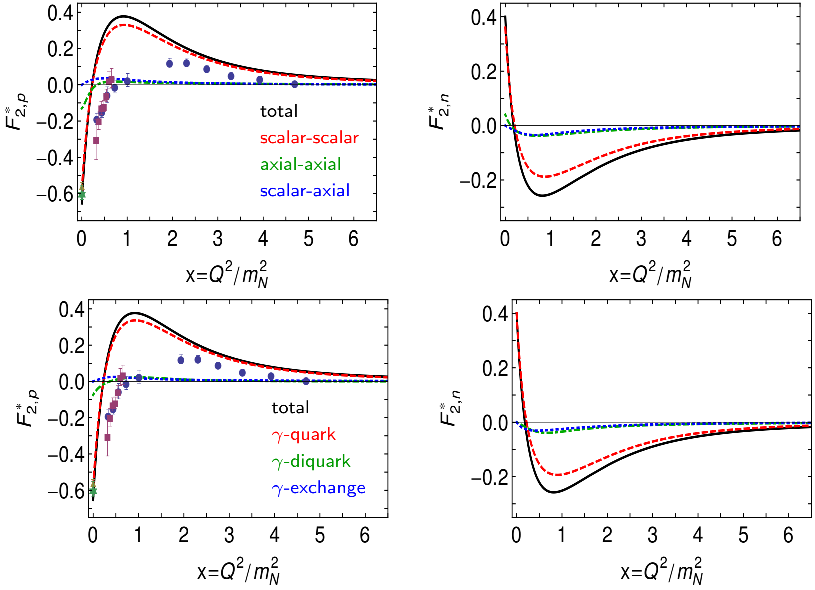

C. Chen *et al.*, Phys. Rev. D99 (2019) 034013.

Transition form factors of $\gamma^* N \to \Delta(1232)\frac{3}{2}^+$, $\Delta(1600)\frac{3}{2}^+$

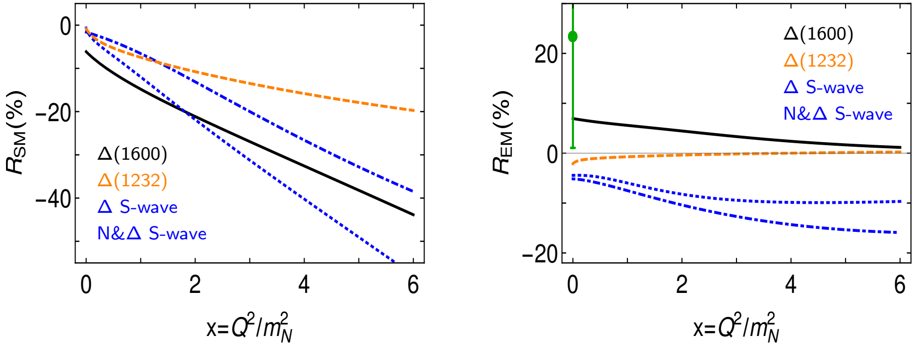

Ya Lu *et al.*, Phys. Rev. D100 (2019) 034001.

☞ Observations:

- R_{SM} and R_{EM} are different from zero indicating that Δ(1232) and Δ(1600) are not simple *S*-wave ground and radial-excitation states of the Δ-baryon.
- R_{SM} and R_{EM} for the Δ(1600) transition are far larger in magnitude than the analogous results for the Δ(1232).
- Points above are an observable manifestation of important higher orbital angular momentum components in both states.
- In particular, there is an enhanced *D*-wave strength in the Δ(1600) relative to that in the Δ(1232).

Epilogue

We have provided a perspective on the contemporary application of continuum functional methods to study strong-QCD in new generation facilities

☞ Advantages:

- Poincaré covariant formulation → Valid for all momentum scales → Access to both perturbative and nonperturbative regimes of QCD.
- Cover full quark mass range → between chiral limit and the heavy quark domain → in an unified way trough a gap equation.
- Ansätze are constrained by symmetry properties, multiplicative renormalizability, perturbative limits, few model parameters usually related with fundamental quantities.

☞ Consequences:

- Existence of dynamical generation of quark- and gluon-mass scales and the saturation at infrared of process-independent effective-charge.
- The features of baryons, and their unification with the properties of mesons, depend on a veracious expression of DCSB in the hadron's bound-state and scattering problems.
- The existence of non-pointlike, fully dynamical quark-quark correlations, as well as quark-gluon and antiquark-gluon ones, is an important consequence of DCSB.